2015

Distinguishing LSP archetypes via gluino pair production at LHC13

Baris Altunkaynak
University of Oklahoma, baris@nhn.ou.edu

Howard Baer
University of Oklahoma, baer@nhn.ou.edu

Vernon Barger
University of Wisconsin, barger@pheno.wisc.edu

Peisi Huang
University of Chicago, peisi.huang@unl.edu

Follow this and additional works at: http://digitalcommons.unl.edu/physicsfacpub

Distinguishing LSP archetypes via gluino pair production at LHC13

Baris Altunkaynak,[1,*] Howard Baer,[1,†] Vernon Barger,[2,‡] and Peisi Huang[3,4,§]

[1]*Homer L. Dodge Department of Physics and Astronomy, University of Oklahoma,*
Norman, Oklahoma 73019, USA
[2]*Department of Physics, University of Wisconsin, Madison, Wisconsin 53706, USA*
[3]*The Enrico Fermi Institute, University of Chicago, Chicago, Illinois 60637, USA*
[4]*HEP Division, Argonne National Laboratory, Argonne, Illinois 60439, USA*

The search for supersymmetry at run 1 of the LHC has resulted in gluino mass limits $m_{\tilde{g}} \gtrsim 1.3$ TeV for the case where $m_{\tilde{q}} \gg m_{\tilde{g}}$ and in models with gaugino mass unification. The increased energy and, ultimately, luminosity of LHC13 will explore the range $m_{\tilde{g}} \sim 1.3$–2 TeV. We examine how the discovery of SUSY via gluino pair production would unfold via a comparative analysis of three LSP archetype scenarios: (1) mSUGRA/CMSSM model with a binolike LSP, (2) charged SUSY breaking (CSB) with a winolike LSP, and (3) SUSY with radiatively driven naturalness (RNS) and a Higgsino-like LSP. In all three cases we expect heavy-to-very-heavy squarks as suggested by a decoupling solution to the SUSY flavor and CP problems and by the gravitino problem. For all cases, initial SUSY discovery would likely occur in the multi-b-jet $+ \not{E}_T$ channel. The CSB scenario would be revealed by the presence of highly ionizing, terminating tracks from quasistable charginos. As further data accrue, the RNS scenario with 100–200 GeV Higgsino-like LSPs would be revealed by the buildup of a mass edge/bump in the opposite sign/same flavor dilepton invariant mass which is bounded by the neutralino mass difference. The mSUGRA/CMSSM archetype would contain neither of these features but would be revealed by a buildup of the usual multilepton cascade decay signatures.

I. INTRODUCTION

The LHC8 (LHC with $\sqrt{s} = 7$–8 TeV) era has come to a close and the LHC13 era is underway. What have we learned from LHC8? The Standard Model (SM) has been spectacularly confirmed in a vast assortment of measurements [1]. And most importantly, a very SM-like Higgs boson has been revealed with mass $m_h = 125.09 \pm 0.24$ GeV (ATLAS/CMS combined) [2,3]. The next major target for LHC is to root out evidence for supersymmetry (SUSY). Indeed, it has been declared that if LHC13 does not uncover evidence for SUSY early within run 2, then physics will have entered a state of crisis [4].

What we have learned from LHC8 is that—in generic models such as mSUGRA/CMSSM—no evidence for SUSY translates into mass bounds of

$$m_{\tilde{g}} \gtrsim 1.3 \text{ TeV} \quad \text{for } m_{\tilde{q}} \gg m_{\tilde{g}} \quad \text{and} \tag{1}$$

$$m_{\tilde{g}} \gtrsim 1.8 \text{ TeV} \quad \text{for } m_{\tilde{q}} \sim m_{\tilde{g}}. \tag{2}$$

In addition, the rather large value of $m_h \simeq 125$ GeV seems to require large radiative corrections to m_h^2 in the MSSM [5]. The Higgs mass can be accommodated with TeV-scale

top squarks for large trilinear soft breaking parameter A_0 [6] or by 10–100 TeV top squarks in the minimal mixing case [7]. Naively, these rather high sparticle mass limits seem to conflict with notions of weak-scale naturalness which favor sparticles at or around $m_{\text{weak}} \simeq 100$ GeV, the value of $m_{W,Z,h}$. This has led to some puzzlement as to the emerging little hierarchy: why is $m(sparticle) \gg m_{\text{weak}}$? It has also led to more detailed examination of what is meant by electroweak naturalness.

The point of contact between SUSY Lagrangian mass parameters (soft terms and superpotential μ term) and hard data occurs in the scalar (Higgs) potential: in the MSSM, it is given by

$$V_{\text{Higgs}} = V_{\text{tree}} + \Delta V, \tag{3}$$

where the tree-level portion is given by

$$V_{\text{tree}} = (m_{H_u}^2 + \mu^2)|h_u^0|^2 + (m_{H_d}^2 + \mu^2)|h_d^0|^2 \\ - B\mu(h_u^0 h_d^0 + \text{H.c.}) + \frac{1}{8}(g^2 + g'^2)(|h_u^0|^2 - |h_d^0|^2)^2 \tag{4}$$

and the radiative corrections (in the effective potential approximation) by

$$\Delta V = \sum_i \frac{(-1)^{2s_i}}{64\pi^2} \text{Tr}\left((\mathcal{M}_i \mathcal{M}_i^\dagger)^2 \left[\log \frac{\mathcal{M}_i \mathcal{M}_i^\dagger}{Q^2} - \frac{3}{2} \right] \right), \tag{5}$$

*baris@nhn.ou.edu
†baer@nhn.ou.edu
‡barger@pheno.wisc.edu
§peisi@uchicago.edu

where the sum over i runs over all fields that couple to Higgs fields, $\mathcal{M}_i^2$ is the Higgs field dependent mass squared matrix (defined as the second derivative of the tree-level Lagrangian) of each of these fields, and the trace is over the internal as well as any spin indices. Minimization of the scalar potential in the h_u^0 and h_d^0 directions allows one to compute the gauge boson masses in terms of the Higgs field vacuum expectation values v_u and v_d, and leads to the well-known condition that

$$\frac{m_Z^2}{2} = \frac{(m_{H_d}^2 + \Sigma_d^d) - (m_{H_u}^2 + \Sigma_u^u)\tan^2\beta}{(\tan^2\beta - 1)} - \mu^2, \quad (6)$$

where the Σ_u^u and Σ_d^d terms arise from derivatives of ΔV evaluated at the potential minimum and $\tan\beta \equiv \frac{v_u}{v_d}$. This minimization condition relates the Z-boson mass scale to the soft SUSY breaking terms and the superpotential Higgsino mass μ. In most computations of the SUSY mass spectrum, the weak-scale soft terms are determined by renormalization group running from a constrained set of parameters set at some high scale Λ. In gravity mediation [8], Λ is usually taken to be $m_{\rm GUT} \simeq 2 \times 10^{16}$ GeV [9]. Then the weak-scale value of μ is dialed (fine-tuned) so that the measured value of m_Z is obtained. An evaluation of the extent of this fine-tuning is provided by the electroweak measure Δ_{EW} which evaluates the largest of the 43 terms on the right-hand side of Eq. (6). If one term on the rhs is $\gg m_Z^2$, then some other unrelated term will have to be large and of opposite-sign to guarantee that $m_Z = 91.2$ GeV. To avoid such large weak-scale tuning, evidently all terms on the right-hand side of Eq. (6) should be comparable to or less than m_Z^2. This implies the following [10,11]:

(i) The superpotential Higgsino mass $\mu \sim 100$–200 GeV, the closer to m_Z the better. The lower limit $\mu \gtrsim 100$ GeV comes from null searches for chargino pair production at LEP2.

(ii) The soft term $m_{H_u}^2$ is radiatively driven to small values $\sim -m_Z^2$ at the weak scale.

(iii) The radiative corrections Σ_u^u are not too large. The largest of these usually comes from the top-squarks. Each of the terms $\Sigma_u^u(\tilde{t}_{1,2})$ are minimized by TeV-scale highly mixed top squarks, a condition which also lifts m_h up to ~ 125 GeV [10,11].

Some alternative fine-tuning measures also have been advocated in the literature.

(1) The usual application of the Higgs mass large-log measure $\Delta_{HS} = \delta m_{H_u}^2/(m_h^2/2)$ where $\delta m_{H_u}^2 \sim \frac{f_t^2}{8\pi^2}(m_{Q_3}^2 + m_{U_3}^2 + A_t^2) \ln(\Lambda/m_{\rm SUSY})$ has been challenged [12,13] in that it ignores the *dependent* term $m_{H_u}^2$ which occurs in the RGE. However, the larger $m_{H_u}^2(\Lambda)$ becomes, the greater is the cancelling correction to $\delta m_{H_u}^2$ [14]. By appropriately combining dependent terms, Δ_{HS} reduces to the same general consequences as Δ_{EW}.

(2) Alternatively, the Ellis *et al.*/Barbieri-Giudice measure [15,16] is defined as $\Delta_{BG} \equiv \max_i |\partial \ln(m_Z^2)/\partial p_i|$ where the p_i constitute fundamental high-scale parameters of the theory. To evaluate Δ_{BG}, m_Z^2 must be evaluated in terms of fundamental high-scale parameters usually taken to be the GUT-scale soft breaking terms. The usual application of this measure has been challenged [12,13] in that in supergravity theories, the soft terms are not independent but are evaluated as multiples of the fundamental gravitino mass $m_{3/2}$. Evaluating Δ_{BG} in terms of the independent parameters μ and $m_{3/2}$, low Δ_{BG} also leads to the same general consequences as Δ_{EW}.

Using Δ_{EW}, then indeed most constrained high-scale SUSY models are found to be highly tuned in the EW sector [13]. An exception occurs for a pocket of parameter space of the two-extra parameter nonuniversal Higgs models [17] where $\mu \sim 100$–200 GeV and where $m_{H_u}^2$ is driven to small negative values comparable to $-m_Z^2$ while allowing for highly mixed TeV-scale top squarks which provide $m_h \simeq 125$ GeV. This pocket of parameter space we call SUSY with radiatively driven naturalness (RNS). By requiring EW naturalness, then upper bounds can be computed for all sparticle masses [11]. In radiative natural SUSY with $\Delta_{EW} < 10\,(30)$ then it is found that [11]

(i) $m_{\tilde{g}} \lesssim 2.5\,(5)$ TeV,

(ii) $m_{\tilde{t}_1} \lesssim 2\,(3)$ TeV,

(iii) $m_{\tilde{W}_1, \tilde{Z}_{1,2}} \lesssim 200\,(300)$ GeV.

The first of these values can be compared to the ultimate reach of LHC14 with $1000\,{\rm fb}^{-1}$ where a 5σ discovery can be established for $m_{\tilde{g}} \lesssim 2$ TeV [18,19]. Thus, while EW naturalness certainly allows for gluinos and squarks to lie well beyond the ultimate reach of LHC13, it is also true that the *most* natural values of gluino and squark masses are those within the exploratory range of LHC13: the lighter the better. This motivates an examination of how a SUSY discovery via gluino pair production is likely to unfold at LHC13 when the gluino mass lies just beyond the present bounds.

In this paper we assume a gluino mass of $m_{\tilde{g}} = 1400$ GeV, i.e. just beyond present bounds. We then investigate how a SUSY discovery would unfold under three lightest SUSY particle (LSP) archetype scenarios:

(i) the mSUGRA/CMSSM model with a binolike LSP,

(ii) a charged SUSY breaking (CSB) scenario with a winolike LSP and

(iii) SUSY with radiatively driven naturalness and a Higgsino-like LSP.

Our goal is to look for commonalities and differences between these three archetype scenarios that would allow a rapid determination of the nature of the LSP if a gluino pair production signal emerges at LHC13.

Towards this end, in Sec. II, we present three archetype benchmark models (BM) labeled as mSUGRA, CSB and RNS. While each BM model contains a gluino with mass

1400 GeV, their implications for collider searches will be very different. In Sec. III, we discuss how SUSY discovery would unfold in each BM model while in Sec. IV we discuss how each archetype could ultimately be distinguished as more integrated luminosity accrues. Briefly, in all cases the most likely initial discovery channel could occur in the multi-b-jet $+ \not{E}_T$ channel with ~ 3–8 fb^{-1} of integrated luminosity. For the CSB benchmark, the model would be distinguished by the presence of one or more cm-length highly ionizing tracks (HITs) from quasistable charginos which are produced within the gluino cascade decays. For the RNS scenario, as 100–1000 fb^{-1} of integrated luminosity accumulates, then a distinctive opposite-sign/same flavor (OS/SF) dilepton invariant mass edge should develop in multi-b-jet $+ \not{E}_T$ events which contain such a dilepton pair. The mass edge occurs at the kinematic limit $m(\ell^+\ell^-) < m_{\tilde{Z}_2} - m_{\tilde{Z}_1} \sim 10$–30 GeV in RNS models. For the mSUGRA benchmark, neither of the above distinctive features should develop, but instead the usual multilepton plus multijet $+ \not{E}_T$ cascade decay topologies should build up as greater integrated luminosity accrues. Our summary and conclusions are given in Sec. V.

II. BENCHMARK MODELS

In this section, we present three benchmark models representing each of three LSP archetype scenarios. Each scenario contains a light Higgs scalar $m_h \simeq 125$ GeV[1] and a gluino of mass $m_{\tilde{g}} = 1.4$ TeV, just beyond the bounds from LHC8. All spectra were generated using the Isajet/Isasugra 7.84 program [20].

A. mSUGRA/CMSSM

In the minimal supergravity model (mSUGRA or CMSSM) [8], it is assumed that supergravity is broken in a hidden sector leading to a massive gravitino characterized by mass $m_{3/2}$, with $m_{3/2} \sim 1$ TeV in accord with phenomenological requirements. In the limit as $M_P \to \infty$ but keeping $m_{3/2}$ fixed, then one is led to the global SUSY Lagrangian of the MSSM augmented by soft SUSY breaking terms, each of order $m_{3/2}$. A simplifying assumption (with minimal motivation) is that all soft scalar masses are unified to m_0 at the GUT scale. In addition, all gaugino masses are unified to $m_{1/2}$, all trilinears are unified to A_0 and there is a bilinear term B. Renormalization group running connects the GUT-scale parameters to the weak-scale ones. At the weak scale, the scalar potential is minimized and the superpotential μ parameter is dialed (fine-tuned) so as to generate the measured value of $m_Z = 91.2$ GeV.

Spectra from this popular model [21–24] can be generated with many computer codes. In Table I, we show a mSUGRA benchmark model with $m_0 = 5$ TeV, $m_{1/2} = 517$ GeV, $A_0 = -8$ TeV and the ratio of Higgs vevs $\tan\beta = 10$. These parameters lead to a spectra with a gluino mass $m_{\tilde{g}} = 1.4$ TeV, i.e. just beyond the reach of LHC8. The light Higgs mass $m_h = 123.6$ GeV, in accord with its measured value if one allows for the ± 2 GeV uncertainty in our calculation of m_h. The $\tilde{Z}_1$ is a binolike LSP. The superpotential μ parameter turns out to be $\mu = 2861$ GeV leading to $\Delta_{EW} = 1968$, so that this benchmark is highly fine-tuned in the EW sector. The calculated thermal neutralino abundance $\Omega_{\tilde{Z}_1}^{TP} h^2 = 317$ is far beyond the measured value. Thus, some sort of (1) late entropy dilution, (2) decay of $\tilde{Z}_1$ to an even lighter LSP such as an axino or (3) R-parity violating decays of $\tilde{Z}_1$ would need to be invoked to bring the model into accord with the measured dark matter density. A schematic illustration of the lighter spectral states of the mSUGRA benchmark is shown in Fig. 1.

B. Charged SUSY breaking

In models labeled as minimal anomaly-mediation (mAMSB) [25], it is assumed that SUSY is broken in a secluded sector so that the dominant contributions to soft terms come not from tree-level supergravity but from the superconformal anomaly. Such models leads characteristically to spectra including winolike gauginos as the lightest SUSY particles [26]. Further, one obtains spectra with well-known tachyonic sleptons. In the original construct [25], it was suggested to augment soft scalar masses with a common m_0^2 term to cure the tachyon problem.

The original mAMSB models seem disfavored in that they have problems generating $m_h \simeq 125$ GeV due to a rather small weak-scale A_t soft term [7,27]. An alternative incarnation goes under the label of PeV SUSY [28], split SUSY [29], pure gravity mediation [30] and spread SUSY [31]. In the simple yet elegant construction of Wells [28], it is argued that the PeV scale (with $m(\text{scalars}) \sim m_{3/2} \sim 1$ PeV $= 1000$ TeV) is motivated by considerations of wino dark matter and neutrino mass while providing a decoupling solution [32] to the SUSY flavor, CP, proton decay and gravitino/moduli problems. This model invoked "charged SUSY breaking" (CSB) where the hidden sector superfield S is charged under some unspecified symmetry. In such a case, the scalars gain masses via SUGRA,

$$\int d^2\theta d^2\bar{\theta} \frac{S^\dagger S}{M_P^2} \Phi_i^\dagger \Phi_i \Rightarrow \frac{F_S^\dagger F_S}{M_P^2} \phi_i^* \phi_i, \qquad (7)$$

while gaugino masses, usually obtained via gravity mediation as

$$\int d^2\theta \frac{S}{M_P} WW \Rightarrow \frac{F_s}{M_P} \lambda\lambda, \qquad (8)$$

---

[1]We allow for a $\sim \pm 2$ GeV theory uncertainty on the Isajet RG-improved one-loop effective potential calculation of m_h, which includes leading two-loop terms [5].
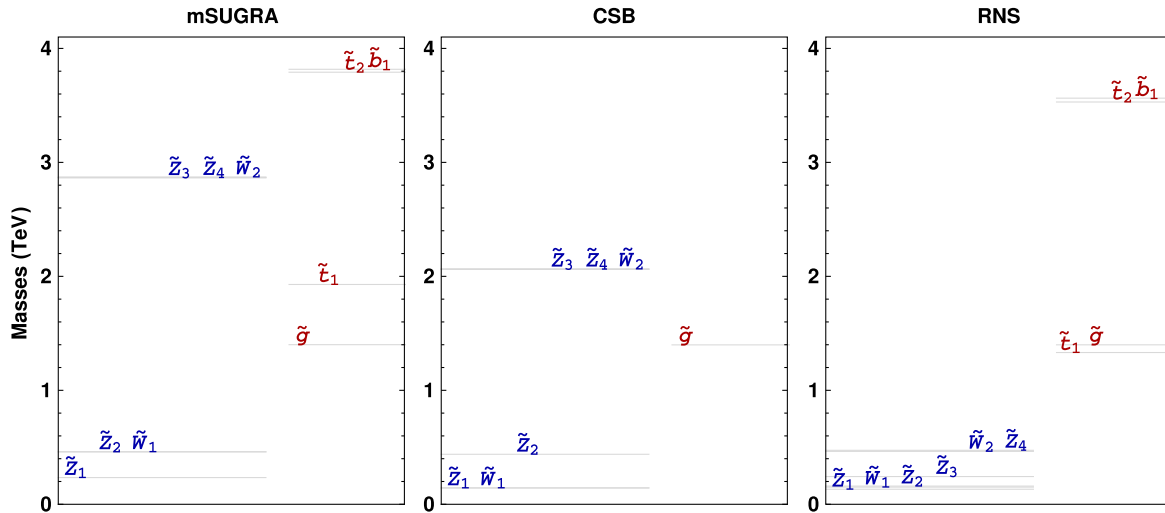
FIG. 1 (color online). Spectra of benchmark models: mSUGRA (left), CSB (middle), RNS (right). We display the bottom part of the spectra up to 4 TeV where the electroweak -inos are shown in blue while the gluinos, stops and sbottoms are shown in red. The sparticles within the same column are ordered in increasing mass from left to right. In the CSB model, the stop and sbottom masses are ~35 TeV: see Table I.

are now forbidden. Then the dominant contribution to gaugino masses comes from AMSB:

$$M_1 = \frac{33}{5} \frac{g_1^2}{16\pi^2} m_{3/2} \sim m_{3/2}/120, \qquad (9)$$

$$M_2 = \frac{g_2^2}{16\pi^2} m_{3/2} \sim m_{3/2}/360, \qquad (10)$$

$$M_3 = -3 \frac{g_3^2}{16\pi^2} m_{3/2} \sim -m_{3/2}/40. \qquad (11)$$

Saturating the measured dark matter abundance with thermally produced (TP) winos requires $m_{\tilde{W}} \sim M_2 \sim 2.5$ TeV which in turn requires the gravitino and scalar masses to occur at the ~1000 TeV (1 PeV) level. A virtue of the CSB model is that the highly massive top squarks $m_{\tilde{t}_{1,2}} \sim 50$–100 TeV lead to $m_h \sim 125$ GeV even with a tiny A_t trilinear soft term.

The CSB benchmark point is listed in Table I where $m_0 \simeq m_{3/2} = 50.57$ TeV leading to squark and slepton masses ~50 TeV but with $m_{\tilde{g}} = 1.4$ TeV. The LSP is a winolike neutralino $\tilde{Z}_1$ with mass $m_{\tilde{Z}_1} = 143.4$ GeV. The superpotential μ parameter is taken to be 2 TeV. The dominant contribution to the EW fine-tuning measure Δ_{EW} comes from the top squark radiative corrections leading to $\Delta_{EW} = 5228$ so the model is highly fine-tuned in the EW sector. The thermally produced winolike neutralino abundance is found from IsaReD [33] to be $\Omega_{\tilde{Z}_1}^{TP} = 0.0013$ so WIMPs are thermally underproduced. They could be augmented via nonthermal WIMP production (e.g. from gravitino, axino, saxion or moduli decays [34]) or the DM abundance could be augmented by other species such as

axions [35]. The CSB benchmark is also shown schematically in Fig. 1.

C. SUSY with radiatively driven naturalness (RNS)

In models with radiatively driven naturalness, it is assumed that soft terms arise via gravity mediation and

TABLE I. Input parameters and masses (in GeV) for three benchmark points computed with ISAJET 7.84 [20]. Also displayed are the bino, wino and Higgsino fractions.

	mSUGRA	CSB	RNS
m_0	5,000	50,570	5,000
M_1	517.0	927.3	517.8
M_2	517.0	140.5	517.8
M_3	517.0	−421.5	517.8
A_0	−8,000	140.5	−8,000
$\tan\beta$	10	10	10
μ	2,861	2,000	150
m_A	5,666	2,000	2,000
m_h	123.6	126.4	124.1
$m_{\tilde{g}}$	1,400	1,399	1,399
$m_{\tilde{u}_L}$	5,065	50,205	5,038
$m_{\tilde{t}_1}$	1,929	34,327	1,332
$m_{\tilde{W}_2}$	2,872.0	2,064.8	464.3
$m_{\tilde{W}_1}$	460.8	143.6	150.7
$m_{\tilde{Z}_4}$	2,866.3	2,062.8	473.6
$m_{\tilde{Z}_3}$	2,865.1	2,062.2	243.3
$m_{\tilde{Z}_2}$	459.8	438.8	159.5
$m_{\tilde{Z}_1}$	234.3	143.4	132.1
Bino frac.	0.9999	0.0022	0.2915
Wino frac.	0.0010	0.9993	0.1747
Higgsino frac.	0.0151	0.0365	0.9405
$\Omega_{\tilde{Z}_1}^{TP} h^2$	317	0.0013	0.01
Δ_{EW}	1968	5228	10.4

are characterized by the scale $m_{3/2} \sim 2\text{--}20$ TeV. Such heavy soft terms lead to $m_h \simeq 125$ GeV for highly mixed TeV-scale top squarks. The μ parameter arises differently. In the SUSY DFSZ axion model [36,37], the Higgs multiplets $\hat{H}_u$ and $\hat{H}_d$ are assigned PQ charges so that the usual μ term is forbidden although now the Higgs superfields may couple to additional gauge singlets from the PQ sector. The μ term is then regenerated via PQ symmetry breaking at a value of $\mu \sim f_a^2/M_P$ so that the little hierarchy $\mu \ll m_{3/2}$ is merely a reflection of the mismatch between the PQ breaking scale and hidden sector mass scale $f_a \ll m_{\text{hidden}}$. In the MSY SUSY axion model [38], the PQ symmetry is broken radiatively as a consequence of SUSY breaking in a similar manner that EW symmetry is radiatively broken as a consequence of SUSY breaking. The radiative PQ breaking generates a small $\mu \sim 100\text{--}200$ GeV (as required by naturalness) from multi-TeV values of $m_{3/2}$ [39]. Once μ is known, then the weak-scale value of $m_{H_u}^2$ is determined by the scalar potential minimization condition and is also of order $-m_Z^2$ as required by naturalness. The weak-scale value of $m_{H_u}^2$ is evolved to m_{GUT} where it is found that $m_{H_u}(m_{\text{GUT}}) \neq m_0$, where m_0 now labels just the matter scalar masses.

The RNS benchmark model is shown in Table I with matter scalar mass $m_0 = 5$ TeV and a trilinear soft term $A_0 = -8$ TeV. The ratio of Higgs vevs $\tan\beta = 10$ and the pseudoscalar Higgs mass m_A is taken as 2 TeV. The unified gaugino mass $m_{1/2} = 517.8$ GeV leading to $m_{\tilde{g}} = 1.4$ TeV. The highly mixed top squarks with mass $m_{\tilde{t}_{1,2}} = 1.3(3.5)$ TeV lead to $m_h = 124.1$ GeV. Since $\mu = 150$ GeV, then the model has $\Delta_{EW} = 10.4$ or about 10% fine-tuning in the EW sector: the model is very natural. The LSP is a Higgsino-like WIMP with mass $m_{\tilde{Z}_1} = 132.1$ GeV. The TP relic density $\Omega_{\tilde{Z}_1}^{TP} h^2 = 0.01$ but in this case the axion could comprise the bulk of DM [40].[2] The RNS benchmark is schematically shown as the third frame of Fig. 1.

III. HOW SUSY DISCOVERY UNFOLDS

A. Gluino pair production

In the benchmark scenarios we have selected, a heavy spectrum of matter scalars–squarks and sleptons–is assumed. This is in accord with at least a partial decoupling solution to the SUSY flavor, CP, gravitino and proton-decay problems. In addition, to accommodate Affleck-Dine [42] leptogenesis, then a nonflat Kähler metric is required [43] from which one would expect generic flavor and CP violation. The decoupling solution allows the AD mechanism to proceed in the face of potential flavor violations.

---

[2]An alternative way to match the measured DM density is to reduce the bino mass M_1 for the case of gaugino mass nonuniversality; see [41].
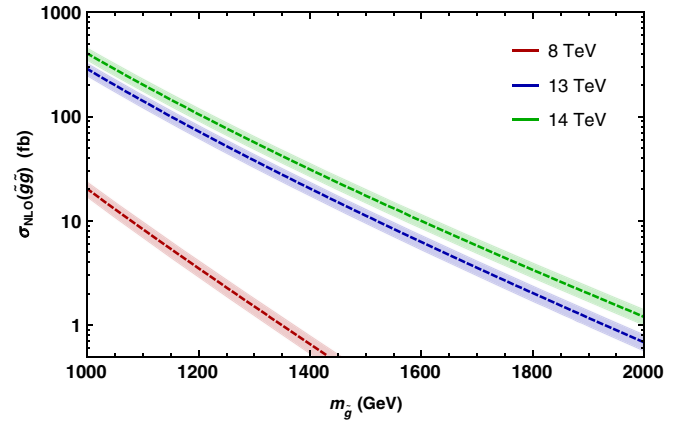

FIG. 2 (color online). Gluino pair production cross section at the LHC for $\sqrt{s} = 8$, 13, 14 TeV calculated at NLO with PROSPINO [44]. Squarks are assumed to be heavy with mass $m_{\tilde{q}} = 5$ TeV. The shaded areas show the scale uncertainty.

In the case of decoupled matter scalars, then we expect gluino pair production and possibly electroweak -ino pair production to offer the main SUSY discovery reactions. In Fig. 2, we show the NLO values of $\sigma(pp \to \tilde{g}\tilde{g}X)$ reaction versus $m_{\tilde{g}}$ for $\sqrt{s} = 8$, 13 and 14 TeV. The squark masses have been set to 5 TeV. We use PROSPINO to calculate the total cross sections [44].

For our benchmark points with $m_{\tilde{g}} = 1.4$ TeV, we see that the LHC8 total production cross section $\sigma(\tilde{g}\tilde{g})$ is about 0.6 fb. As $\sqrt{s}$ is increased to 13 TeV for LHC Run 2, then the total gluino pair production cross section jumps by a factor of ~ 30 to $\simeq 20$ fb. Future LHC runs with fully trained magnets may attain $\sqrt{s} \sim 14$ TeV for which $\sigma(\tilde{g}\tilde{g})$ would rise to ~ 35 fb. While EW -ino pair production rates should be comparable to gluino pair production—due to their lower masses—we expect at this stage that gluino pair production is more easily seen due to its large energy release and no cost for leptonic branching fractions in the major signal channel of jets $+ \not{E}_T$.

B. Gluino branching fractions and signatures

Once produced, the gluinos can cascade decay [45] to a variety of final states which are listed in Table II. The decay modes including q in the final state are summed over $q = u, d, s, c$ possibilities. It is evident from the table that in all cases the decays to third-generation quarks are enhanced over first- and second-generation quarks. Gluino three-body decays to third generation quarks were first calculated in Refs. [46–48] where their enhancement was noticed to arise from (1) couplings which include the large b and t Yukawa couplings, (2) generically smaller mediator masses $m_{\tilde{t}_{1,2}} \lesssim m_{\tilde{q}}$ and (3) large L-R mixing effects. For our benchmark models, we see that in mSUGRA, the $\tilde{g}$ decays to states including $b\bar{b}$ (both directly and via decay to top followed by $t \to bW$) 81% of the time, while for CSB it is 47% and for RNS it is 99.1%. Thus, for $\tilde{g}\tilde{g}$, we usually

TABLE II.   Gluino branching fractions for the three benchmark models where $q = u$, d, c and s.

final state	mSUGRA	CSB	RNS
$q\bar{q}'\tilde{W}_1$	10.5%	34.0%	0.1%
$tb\tilde{W}_1$	13.4%	28.8%	45.6%
$tb\tilde{W}_2$	$\cdots$%	$\cdots$%	2.2%
$q\bar{q}\tilde{Z}_1$	3.1%	17.0%	$\cdots$%
$b\bar{b}\tilde{Z}_1$	0.5%	8.7%	$\cdots$%
$t\bar{t}\tilde{Z}_1$	60.3%	6.2%	17.2%
$q\bar{q}\tilde{Z}_2$	5.2%	2.4%	$\cdots$%
$b\bar{b}\tilde{Z}_2$	4.3%	0.3%	$\cdots$%
$t\bar{t}\tilde{Z}_2$	2.5%	3.0%	22.5%
$t\bar{t}\tilde{Z}_3$	$\cdots$%	$\cdots$%	10.6%
$t\bar{t}\tilde{Z}_4$	$\cdots$%	$\cdots$%	1.0%

expect the presence of four b jets in the final state (although some of these may fall below acceptance cuts or be merged with other b jets, etc.). In the CSB case, the branching to t and b quarks is only mildly enhanced since all six squark flavors are extremely heavy. In addition, in the mSUGRA and CSB cases, gluinos only decay substantially to the lighter -ino states $\tilde{W}_1$ and $\tilde{Z}_{1,2}$. For the RNS case, gluino decays to the light Higgsino-like EWinos dominates but also decays to the heavier bino- and winolike states $\tilde{Z}_{3,4}$ and $\tilde{W}_2$ can be substantial.

A diagram depicting gluino pair production followed by typical three-body decays is shown in Fig. 3. The presence of up to four b jets in the final state can be used as a powerful veto against dominant SM backgrounds such as $t\bar{t}$ production. Indeed, ATLAS searches [49] for $\tilde{g}\tilde{g}$ production with ≥ 3 b jets in the final state offers the most powerful probe of gluino masses in the case where $m_{\tilde{g}} \ll m_{\tilde{q}}$.

C. Gluino cascade decay signatures

We use Isajet 7.84 [20] to generate a SUSY Les Houches Accord [50] (SLHA) file for each benchmark scenario which is fed into Pythia [51] for generation of gluino pair production events followed by cascade decays. The gluino
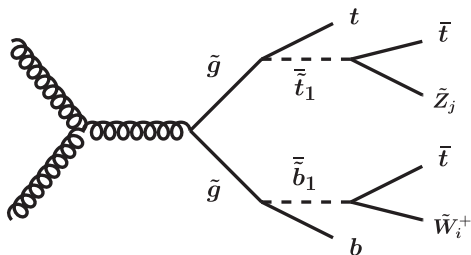
FIG. 3.   Gluino pair production and decay to multiple b jets in the three benchmark scenarios.

pair cross section is normalized to the NLO Prospino results of Fig. 2. We use the Snowmass SM background event set [52] for the background processes. The $t\bar{t}$ background set is expected to be the dominant background [53], where extra b jets can arise from initial or final state radiation and from jet mistags. While the Snowmass background set was generated for $\sqrt{s} = 14$ TeV LHC collisions, we have rescaled the rates for $\sqrt{s} = 13$ TeV collisions. Our signal and BG events are passed through the Delphes [54] toy detector simulation as set up for Snowmass analyses.

We apply the following event selection cuts:
  (i) $n(\text{jets}) \geq 4$,
  (ii) $n(b - \text{jets}) \geq 3$,
  (iii) $E_T(j_1, j_{2-4}) > 100, 50$ GeV,
  (iv) for isolated leptons, then $p_T(\ell) > 20$ GeV,
  (v) $\not{E}_T > \not{E}_T(\text{cut}) = 50, 100\text{–}500$ GeV
  (vi) $A_T > 1200$ GeV,
where $A_T = \not{E}_T + \sum_{\text{leptons}} E_T + \sum_{\text{jets}} E_T$ and for later use $M_{\text{eff}} = \not{E}_T + \sum_{i=1}^{4} E_T(j_i)$. To gain some optimization of signal-to-background (S/B), we tried the above range of $\not{E}_T$ cuts and evaluated S/B with and without the A_T cut.

The cross sections after cuts for various multilepton $+ \geq$ 3 $b$jets $+ \not{E}_T$ channels are shown in Fig. 4. The optimal $\not{E}_T$ cut for the 0ℓ and 1ℓ channels was the hardest value: $\not{E}_T > 500$ GeV. For the opposite sign same flavor (OSSF) dilepton channel, the best cut was $\not{E}_T > 400$ GeV while for the same sign (SS)-dilepton, 3ℓ and 4ℓ channels, the $\not{E}_T > 50$ GeV was best. The $A_T > 1200$ GeV cut helped just marginally.

We see, from Fig. 4, that the signal cross sections after cuts in the jets $+ \not{E}_T$ (0ℓ) channel are 1.9, 3.3 and 2.1 fb, respectively, for the mSUGRA, CSB and RNS cases while SM BG lies at 1.2 fb. In Fig. 5, we show the required value of LHC13 integrated luminosity which is needed to establish a 5σ signal, where in addition we also require at least ten total signal events. From this plot, we see that
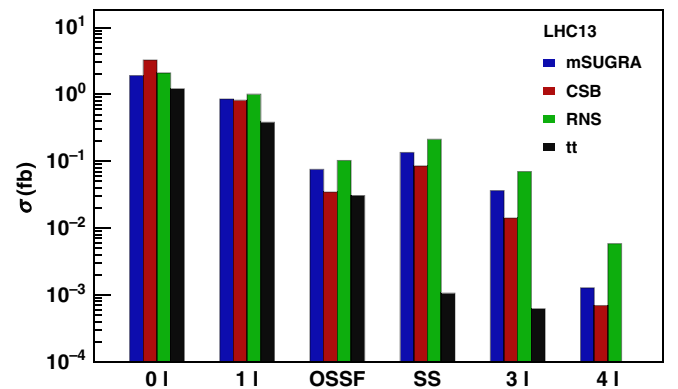
FIG. 4 (color online).   Cross section after cuts from gluino pair production for the three SUSY benchmark models and from $t\bar{t}$ background. For the 0 and 1ℓ signals, we take $\not{E}_T > 500$ GeV while for the OSSF dilepton channel we take $\not{E}_T > 400$ GeV. For the SS, 3ℓ and 4ℓ signals, we require $\not{E}_T > 50$ GeV.
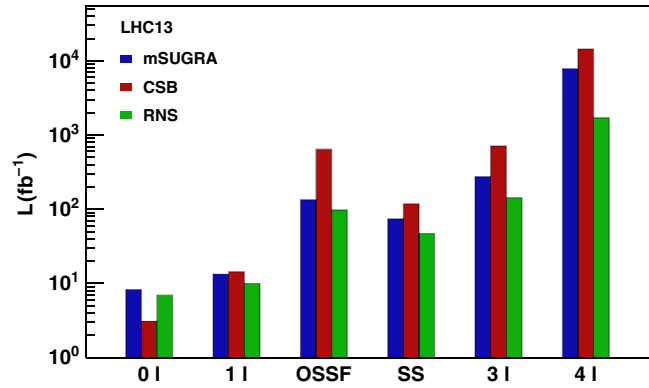
FIG. 5 (color online).   Required integrated luminosity at LHC13 to establish a 5σ SUSY discovery in various channels from gluino pair production for the three SUSY benchmark models compared to $t\bar{t}$ background. For the 0 and 1ℓ signals, we take $E_T >$ 500 GeV while for the OSSF dilepton channel we take $E_T >$ 400 GeV. For the SS, 3ℓ and 4ℓ signals, we require $E_T >$ 50 GeV.

just 8.3, 3.1 or 6.9 fb^{-1} of integrated luminosity L is needed to establish a first signal for the mSUGRA, CSB and RNS benchmark models with $m_{\tilde{g}} = 1.4$ TeV. The CSB benchmark model has a somewhat larger signal cross section and hence requires somewhat lower L in the 0ℓ channel as compared to the mSUGRA and RNS models since its decay modes include more hadronic and fewer leptonic cascades.

In Fig. 4, we also see the cross section after cuts for the 1ℓ channel. Even though one takes a leptonic branching fraction hit in this channel, the numerous sources for a single additional isolated lepton lead to cross sections after cuts which are comparable to those in the 0ℓ channel. For the 1ℓ channel, RNS has the largest cross section 1.0 fb while mSUGRA and CSB are at the 0.8 fb level. This $1\ell + jets + E_T$ channel will confirm the signal which is already established in the 0ℓ channel with just a few additional (10–14) fb^{-1} of integrated luminosity.

In Figs. 4 and 5, we also show the cross section after cuts and the required integrated luminosity for a 5σ signal for the OSSF, SS, 3ℓ and 4ℓ channels. These multilepton channels all exhibit a greater suppression due to multiple leptonic branching fractions as compared to the 0ℓ channel. For the 3ℓ channel, background events come from isolated leptons in the b-quark decays. With the requirement of at least three b jets, we do not observe any events in our $t\bar{t}$ background for the 4ℓ channel. Also, in the multilepton channels, we see that the RNS model yields the largest cross sections due to the large gluino branching fractions into tops followed by $t \to bW$ and $W \to \ell\nu$ decay. From Fig. 5, we see that typically ~ 100 fb^{-1} is necessary to establish a signal in the dilepton and trilepton channels while $\sim 10^3 - 10^4$ fb^{-1} would be required for a 5σ signal in the $4l$ channel.

IV. ESTABLISHING THE LSP ARCHETYPE

A. Charged SUSY breaking

One of the features of the CSB model is that $\tilde{W}_1$ and the LSP are almost degenerate with a mass difference $\Delta m = m_{\tilde{W}_1} - m_{\tilde{Z}_1} \gtrsim m_{\pi^\pm}$. $\tilde{W}_1$ decays into charged pions at almost 100% rate. The reduced phase space also makes the chargino long-lived so that, once produced at the interaction vertex, it travels a visible distance before it decays to soft pions plus the LSP. Since the chargino is so massive, its velocity is borderline relativistic leading to a highly ionizing trail or track (HIT). The chargino lifetime $\tau_{\tilde{W}_1}$ is extracted from Isajet and the actual lifetime of each chargino is generated from the exponential decay law $e^{-t/\tau_{\tilde{W}_1}}$. Then the track length is computed from $d = \beta\gamma t$.

In Fig. 6, we display the histogram of the distance travelled from the interaction vertex to the decay point of each chargino. Here, we see that the typical length of each HIT is of order 2–20 cm. We also display the percentage of events containing 0–2 charginos. We see that 90% of the events passing our cuts contain either one or two charginos in each event. The presence of one or more HITs in candidate SUSY events would be the smoking gun signature of SUSY models with a winolike LSP.

B. Radiatively driven naturalness (RNS)

In the RNS benchmark model, it is emphasized [10,19,55] that the mass gap between the $\tilde{Z}_2$ and $\tilde{Z}_1$ neutralinos is typically small: ~ 10–30 GeV which gives the inter-Higgsino splitting. For our benchmark case, the value is $\Delta m = m_{\tilde{Z}_2} - m_{\tilde{Z}_1} = 27.4$ GeV. Notice this mass gap never gets much below about 10 GeV since naturalness also provides upper bounds to the gaugino masses via loop effects so that the Higgsino-gaugino mass gap cannot become arbitrarily large. The modest $\tilde{Z}_2$-$\tilde{Z}_1$ mass gap has important consequences for phenomenology. It means that the $\tilde{Z}_2$ always decays via 3-body modes $\tilde{Z}_2 \to \tilde{Z}_1 f\bar{f}$
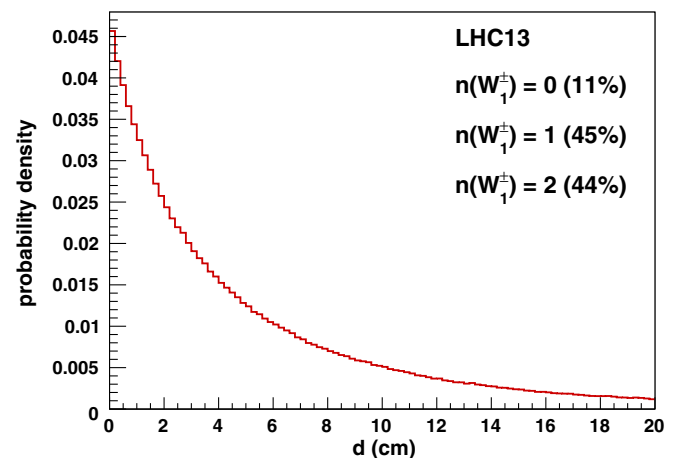

FIG. 6 (color online).   Distance to the decay point from the interaction vertex for the CSB benchmark model.
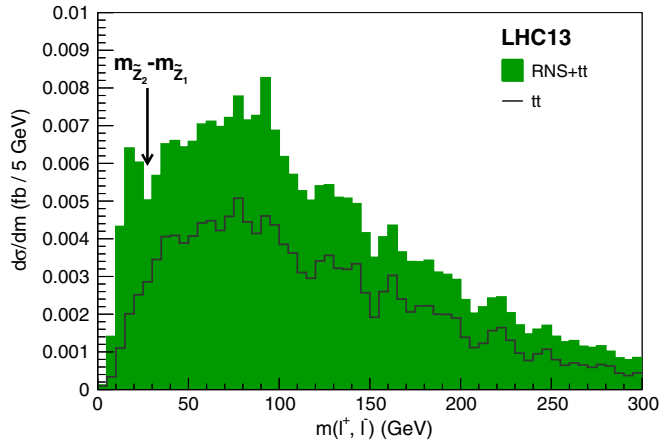
FIG. 7 (color online). Invariant mass of OSSF leptons. The dilepton mass edge and the Z peak are visible for the RNS model. We require $n(b - \text{jets}) \geq 3$.

which is dominated by Z^* exchange. The decay mode $\tilde{Z}_2 \to \tilde{Z}_1 \ell^+ \ell^-$ occurs at 3%–4% per lepton species, but the OSSF dilepton pair which emerges from this decay always has invariant mass kinematically bounded by $m_{\tilde{Z}_2} - m_{\tilde{Z}_1}$. This mass edge should be apparent in gluino pair cascade decay events which contain an OSSF dilepton pair.

In Fig. 7, we show the invariant mass distribution of OSSF dilepton pairs in gluino pair cascade decay events where we require the above cuts but with $\not{E}_T > \max(100 \text{ GeV}, 0.2 M_{\text{eff}})$ and $A_T > 1200 \text{ GeV}$ and the presence of an isolated OSSF dilepton pair. The black histogram shows the expected continuum background distribution arising mainly from $t\bar{t}$ production while the green histogram shows signal plus BG for the RNS benchmark model. The RNS signal is characterized by the distinct mass bump and edge below about 30 GeV. This feature provides the smoking gun signature for SUSY models with light Higgsinos [19]. One can also see a peak at $m(\ell^+ \ell^-) \sim m_Z$ which arises from $\tilde{W}_2$ and $\tilde{Z}_{3,4}$ two-body

decays to a real Z. The area under the $m(\ell^+ \ell^-) < 30 \text{ GeV}$ portion is ~ 0.025 fb so that of order 400 fb^{-1} of integrated luminosity will be required before this feature begins to take shape in real data.

For comparison, in Fig. 8 we show the same $m(\ell^+ \ell^-)$ distribution for the case of the CSB benchmark. In the CSB case, first of all there are far fewer $\ell^+ \ell^-$ pairs present above background, and second there is no obvious structure to the signal distribution: we expect just a continuum.

The second smoking gun signature for models with a Higgsino LSP is the presence of same-sign diboson (SSdB) events which are from wino pair production [19,56]. In this case, the production reaction is typically $pp \to \tilde{W}_2 \tilde{Z}_4$ followed by $\tilde{W}_2 \to \tilde{W}_1 \tilde{Z}_{1,2}$ and $\tilde{Z}_4 \to \tilde{W}_1^{\pm} W^{\mp}$. The Majorana nature of the $\tilde{Z}_4$ leads to equal amounts of same-sign and opposite sign dilepton events. Note that these SSdB events contain minimal jet activity—only that arising from initial state QCD radiation—as opposed to SS dilepton events from gluino and squark cascade decays which should be rich in the presence of additional high p_T jets.

C. mSUGRA/CMSSM

For the mSUGRA/CMSSM benchmark model with a 1.4 TeV gluino, then we expect the production of the usual multilepton+multi-jet + $\not{E}_T$ cascade decay signatures as shown in Fig. 4. For the case of the mSUGRA benchmark, the mass gap between the winolike $\tilde{Z}_2$ and the binolike $\tilde{Z}_1$ is 225.5 GeV so that the $\tilde{Z}_2 \to \tilde{Z}_1 h$ (spoiler) decay mode is open. This two-body decay dominates the $\tilde{Z}_2$ branching fraction, and so we expect no additional structure in the dilepton invariant mass distribution. The $m(\ell^+ \ell^-)$ distribution for the mSUGRA benchmark point is shown in Fig. 9. While no characteristic dilepton structure is apparent, it may be possible instead to pull out the presence of $h \to b\bar{b}$ decays in the mSUGRA cascade decay events where $m(b\bar{b}) \sim m_h$ [57].
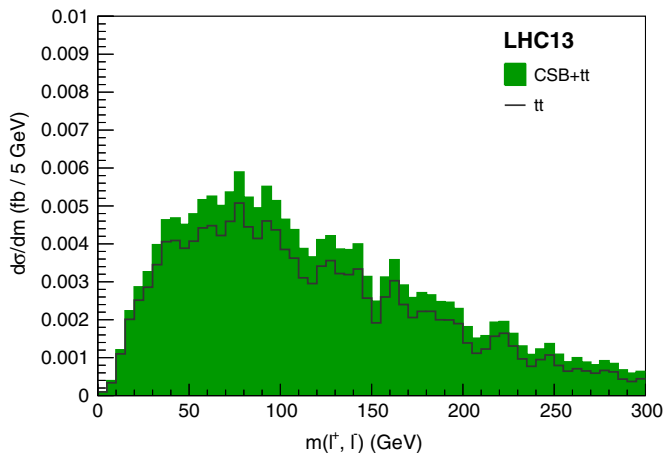

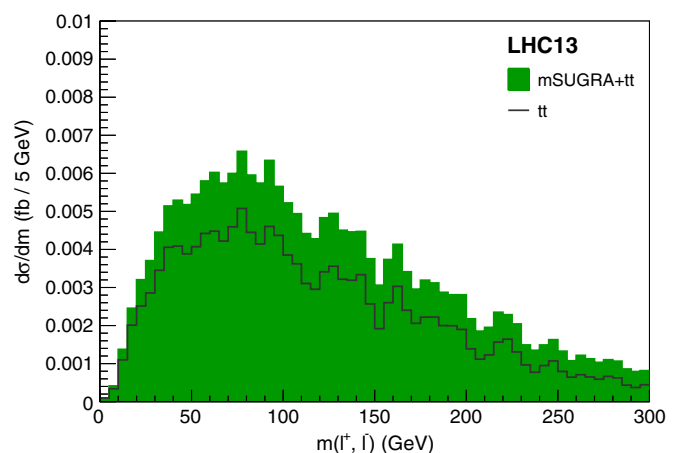FIG. 8 (color online). Invariant mass of OSSF dileptons for the CSB model. We require $n(b - \text{jets}) \geq 3$.

FIG. 9 (color online). Invariant mass of OSSF dileptons for the mSUGRA model. We require $n(b - \text{jets}) \geq 3$.

V. CONCLUSIONS

During run 1 of the LHC at $\sqrt{s} = 7$–8 TeV, the Standard Model was vigorously confirmed in both the electroweak and QCD sectors and the Higgs boson was discovered at $m_h \simeq 125$ GeV. The presence of a bona fide fundamental scalar particle cries out for a mass stabilization mechanism of which the simplest and most elegant one is supersymmetry. Unfortunately, no SUSY particles have yet appeared leading to mass limits for the gluino particle of $m_{\tilde{g}} \gtrsim$ 1.3 TeV.

LHC run 2 with $\sqrt{s} = 13$ TeV has begun. New vistas in SUSY parameter space are open for exploration. While naturalness allows for gluinos as high as 4–5 TeV (with $\Delta_{EW} < 30$), it is yet true that naturalness (mildly via higher order contributions) prefers gluinos as light as possible. Motivated by these circumstances, we considered how SUSY discovery would unfold in three SUSY archetype models with a bino-, wino- and Higgsino-like LSP each with a 1.4 TeV gluino, just beyond present bounds.

We find that SUSY discovery could already arise at the 5σ level with just 3–8 fb^{-1} of integrated luminosity via the $\geq 3b\text{jet} + E_T$ channel. Confirmation would soon follow in the $\geq 3b\text{jet} + 1 - \ell + E_T$ channel. Further confirmation in the 2–3 lepton channels will require ~ 100 fb^{-1}. The CSB benchmark case would immediately be identified by the presence of one or more highly ionizing tracks in each

signal event due to long-lived winolike charginos which undergo delayed decays to a winolike LSP. No such HITs should be apparent in signal events from the mSUGRA or RNS archetype models. Instead, the RNS archtype would be signalled by a gradual buildup of structure in the $m(\ell^+\ell^-)$ OSSF dilepton mass distribution, where the $m(\ell^+\ell^-) < m_{\tilde{Z}_2} - m_{\tilde{Z}_1}$ mass edge along with a Z peak should be apparent with ~ 100–1000 fb^{-1}. In the RNS case, the gluino cascade decay events should ultimately be accompanied by the presence of same-sign diboson events arising from wino pair production.

For the mSUGRA archtype with a binolike LSP, then we expect the usual assortment of gluino-pair-initiated cascade decay multilepton+jets + E_T events but without HITs and without any apparent structure in the $m(\ell^+\ell^-)$ distribution. However, the presence of Higgs bosons lurking within the cascade decay events may be a distinguishing feature. We look forward to data from LHC13.

[1] I. Hinchliffe, in *Proceedings of Phenomenology, 2015, PITTPAC, Pittsburgh.*

[2] G. Aad *et al.* (ATLAS Collaboration), Phys. Lett. B **716**, 1 (2012).

[3] S. Chatrchyan *et al.* (CMS Collaboration), Phys. Lett. B **716**, 30 (2012).

[4] J. Lykken and M. Spiropulu, Sci. Am. **310N5**, 36 (2014).

[5] M. S. Carena and H. E. Haber, Prog. Part. Nucl. Phys. **50**, 63 (2003).

[6] H. Baer, V. Barger, and A. Mustafayev, Phys. Rev. D **85**, 075010 (2012).

[7] A. Arbey, M. Battaglia, A. Djouadi, F. Mahmoudi, and J. Quevillon, Phys. Lett. B **708**, 162 (2012).

[8] H. P. Nilles, Phys. Lett. **115B**, 193 (1982); A. Chamseddine, R. Arnowitt, and P. Nath, Phys. Rev. Lett. **49**, 970 (1982); R. Barbieri, S. Ferrara, and C. Savoy, Phys. Lett. **119B**, 343 (1982); N. Ohta, Prog. Theor. Phys. **70**, 542 (1983); L. Hall, J. Lykken, and S. Weinberg, Phys. Rev. D **27**, 2359 (1983); for an early review, see e.g. H. P. Nilles, Phys. Rep. **110**, 1 (1984); for a recent review, see D. J. H. Chung, L. L. Everett, G. L. Kane, S. F. King, J. D. Lykken, and L. T. Wang, Phys. Rep. **407**, 1 (2005).

[9] R. Arnowitt, A. H. Chamseddine, and P. Nath, Int. J. Mod. Phys. A **27**, 1230028 (2012); see also P. Nath, Phys. Scripta

90, 068007 (2015); H. P. Nilles, Nucl. Phys. B, Proc. Suppl. **101**, 237 (2001).

[10] H. Baer, V. Barger, P. Huang, A. Mustafayev, and X. Tata, Phys. Rev. Lett. **109**, 161802 (2012).

[11] H. Baer, V. Barger, P. Huang, D. Mickelson, A. Mustafayev, and X. Tata, Phys. Rev. D **87**, 115028 (2013).

[12] H. Baer, V. Barger, and D. Mickelson, Phys. Rev. D **88**, 095013 (2013).

[13] H. Baer, V. Barger, D. Mickelson, and M. Padeffke-Kirkland, Phys. Rev. D **89**, 115019 (2014).

[14] H. Baer, V. Barger, and M. Savoy, Phys. Scripta **90**, 068003 (2015).

[15] J. R. Ellis, K. Enqvist, D. V. Nanopoulos, and F. Zwirner, Mod. Phys. Lett. A **01**, 57 (1986).

[16] R. Barbieri and G. F. Giudice, Nucl. Phys. **B306**, 63 (1988).

[17] D. Matalliotakis and H. P. Nilles, Nucl. Phys. **B435**, 115 (1995); P. Nath and R. L. Arnowitt, Phys. Rev. D **56**, 2820 (1997); J. Ellis, K. Olive, and Y. Santoso, Phys. Lett. B **539**, 107 (2002); J. Ellis, T. Falk, K. Olive, and Y. Santoso, Nucl. Phys. **B652**, 259 (2003); H. Baer, A. Mustafayev, S. Profumo, A. Belyaev, and X. Tata, J. High Energy Phys. 07 (2005) 065.

[18] H. Baer, V. Barger, A. Lessa, and X. Tata, Phys. Rev. D **86**, 117701 (2012).

[19] H. Baer, V. Barger, P. Huang, D. Mickelson, A. Mustafayev, W. Sreethawong, and X. Tata, J. High Energy Phys. 12 (2013) 013.

[20] F. E. Paige, S. D. Protopopescu, H. Baer, and X. Tata, arXiv:hep-ph/0312045.

[21] G. G. Ross and R. G. Roberts, Nucl. Phys. **B377**, 571 (1992).

[22] R. L. Arnowitt and P. Nath, Phys. Rev. Lett. **69**, 725 (1992).

[23] V. D. Barger, M. S. Berger, and P. Ohmann, Phys. Rev. D **47**, 1093 (1993).

[24] V. D. Barger, M. S. Berger, and P. Ohmann, Phys. Rev. D **49**, 4908 (1994).

[25] L. Randall and R. Sundrum, Nucl. Phys. **B557**, 79 (1999); G. F. Giudice, M. A. Luty, H. Murayama, and R. Rattazzi, J. High Energy Phys. 12 (1998) 027.

[26] T. Gherghetta, G. F. Giudice, and J. D. Wells, Nucl. Phys. **B559**, 27 (1999); J. L. Feng, T. Moroi, L. Randall, M. Strassler, and S. f. Su, Phys. Rev. Lett. **83**, 1731 (1999).

[27] H. Baer, V. Barger, and A. Mustafayev, J. High Energy Phys. 05 (2012) 091.

[28] J. D. Wells, arXiv:hep-ph/0306127; J. D. Wells, Phys. Rev. D **71**, 015013 (2005).

[29] N. Arkani-Hamed and S. Dimopoulos, J. High Energy Phys. 06 (2005) 073; G. F. Giudice and A. Romanino, Nucl. Phys. **B699**, 65 (2004); **706**, 65(E) (2005); N. Arkani-Hamed, S. Dimopoulos, G. F. Giudice, and A. Romanino, Nucl. Phys. **B709**, 3 (2005).

[30] M. Ibe and T. T. Yanagida, Phys. Lett. B **709**, 374 (2012); M. Ibe, S. Matsumoto, and T. T. Yanagida, Phys. Rev. D **85**, 095011 (2012); B. Bhattacherjee, B. Feldstein, M. Ibe, S. Matsumoto, and T. T. Yanagida, Phys. Rev. D **87**, 015028 (2013); J. L. Evans, M. Ibe, K. A. Olive, and T. T. Yanagida, Eur. Phys. J. C **73**, 2468 (2013); J. L. Evans, M. Ibe, K. A. Olive, and T. T. Yanagida, Eur. Phys. J. C **74**, 2931 (2014); J. L. Evans, M. Ibe, K. A. Olive, and T. T. Yanagida, Phys. Rev. D **91**, 055008 (2015).

[31] L. J. Hall and Y. Nomura, J. High Energy Phys. 01 (2012) 082; L. J. Hall, Y. Nomura, and S. Shirai, J. High Energy Phys. 01 (2013) 036.

[32] M. Dine, A. Kagan, and S. Samuel, Phys. Lett. B **243**, 250 (1990); A. Cohen, D. B. Kaplan, and A. Nelson, Phys. Lett. B **388**, 588 (1996); N. Arkani-Hamed and H. Murayama, Phys. Rev. D **56**, R6733 (1997); T. Moroi and M. Nagai, Phys. Lett. B **723**, 107 (2013).

[33] H. Baer, C. Balazs, and A. Belyaev, J. High Energy Phys. 03 (2002) 042.

[34] T. Moroi and L. Randall, Nucl. Phys. **B570**, 455 (2000).

[35] K. J. Bae, H. Baer, A. Lessa, and H. Serce, arXiv:1502.07198.

[36] M. Dine, W. Fischler, and M. Srednicki, Phys. Lett. B **104**, 199 (1981); A. R. Zhitnitsky, Yad. Fiz. **31**, 497 (1980) [Sov. J. Nucl. Phys. **31**, 260 (1980)].

[37] E. J. Chun, Phys. Rev. D **84**, 043509 (2011); K. J. Bae, E. J. Chun, and S. H. Im, J. Cosmol. Astropart. Phys. 03 (2012) 013; K. J. Bae, H. Baer, and E. J. Chun, J. Cosmol. Astropart. Phys. 12 (2013) 028.

[38] H. Murayama, H. Suzuki, and T. Yanagida, Phys. Lett. B **291**, 418 (1992); T. Gherghetta and G. L. Kane, Phys. Lett. B **354**, (1995) 300; K. Choi, E. J. Chun, and J. E. Kim, Phys. Lett. B **403**, 209 (1997).

[39] K. J. Bae, H. Baer, and H. Serce, Phys. Rev. D **91**, 015003 (2015).

[40] K. J. Bae, H. Baer, and E. J. Chun, Phys. Rev. D **89**, 031701 (2014).

[41] H. Baer, V. Barger, P. Huang, D. Mickelson, M. Padeffke-Kirkland, and X. Tata, Phys. Rev. D **91**, 075005 (2015).

[42] I. Affleck and M. Dine, Nucl. Phys. **B249**, 361(1985).

[43] M. Dine, L. Randall, and S. D. Thomas, Phys. Rev. Lett. **75**, 398 (1995); M. Dine, L. Randall, and S. D. Thomas, Nucl. Phys. **B458**, 291 (1996).

[44] W. Beenakker, R. Hopker, and M. Spira, arXiv:hep-ph/9611232.

[45] H. Baer, J. R. Ellis, G. B. Gelmini, D. V. Nanopoulos, and X. Tata, Phys. Lett. **161B**, 175 (1985); G. Gamberini, Z. Phys. C **30**, 605 (1986); H. Baer, V. D. Barger, D. Karatas, and X. Tata, Phys. Rev. D **36**, 96 (1987); H. Baer, R. M. Barnett, M. Drees, J. F. Gunion, H. E. Haber, D. L. Karatas, and X. R. Tata, Int. J. Mod. Phys. A **02**, 1131 (1987); R. M. Barnett, J. F. Gunion, and H. E. Haber, Phys. Rev. D **37**, 1892 (1988); H. Baer, A. Bartl, D. Karatas, W. Majerotto, and X. Tata, Int. J. Mod. Phys. A **04**, 4111 (1989).

[46] H. Baer, X. Tata, and J. Woodside, Phys. Rev. D **42**, 1568 (1990).

[47] A. Bartl, W. Majerotto, B. Mosslacher, N. Oshimo, and S. Stippel, Phys. Rev. D **43**, 2214 (1991); A. Bartl, W. Majerotto, and W. Porod, Z. Phys. C **64**, 499 (1994).

[48] H. Baer, C. h. Chen, M. Drees, F. Paige, and X. Tata, Phys. Rev. D **58**, 075008 (1998).

[49] G. Aad *et al.* (ATLAS Collaboration), J. High Energy Phys. 10 (2014) 24.

[50] P. Z. Skands, B. C. Allanach, H. Baer, C. Balazs, G. Belanger, F. Boudjema, A. Djouadi, and R. Godbole *et al.*, J. High Energy Phys. 07 (2004) 036.

[51] T. Sjostrand, S. Mrenna, and P. Z. Skands, J. High Energy Phys. 05 (2006) 026.

[52] A. Avetisyan, J. M. Campbell, T. Cohen, N. Dhingra, J. Hirschauer, K. Howe, S. Malik, and M. Narain *et al.*, arXiv:1308.1636.

[53] H. Baer, V. Barger, G. Shaughnessy, H. Summy, and L. t. Wang, Phys. Rev. D **75**, 095010 (2007).

[54] J. de Favereau, J. de Favereau, C. Delaere, P. Demin, A. Giammanco, V. Lemaître, A. Mertens, and M. Selvaggi (DELPHES 3 Collaboration), J. High Energy Phys. 02 (2014) 057.

[55] H. Baer, V. Barger, and P. Huang, J. High Energy Phys. 11 (2011) 031.

[56] H. Baer, V. Barger, P. Huang, D. Mickelson, A. Mustafayev, W. Sreethawong, and X. Tata, Phys. Rev. Lett. **110**, 151801 (2013).

[57] H. Baer, M. Bisset, X. Tata, and J. Woodside, Phys. Rev. D **46**, 303 (1992); H. Baer, C. h. Chen, F. Paige, and X. Tata, Phys. Rev. D **52**, 2746 (1995).